



Benchmark Solutions for Computational Aeroacoustics (CAA) Code Validation

James R. Scott
Glenn Research Center, Cleveland, Ohio

The NASA STI Program Office . . . in Profile

Since its founding, NASA has been dedicated to the advancement of aeronautics and space science. The NASA Scientific and Technical Information (STI) Program Office plays a key part in helping NASA maintain this important role.

The NASA STI Program Office is operated by Langley Research Center, the Lead Center for NASA's scientific and technical information. The NASA STI Program Office provides access to the NASA STI Database, the largest collection of aeronautical and space science STI in the world. The Program Office is also NASA's institutional mechanism for disseminating the results of its research and development activities. These results are published by NASA in the NASA STI Report Series, which includes the following report types:

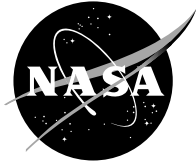
- **TECHNICAL PUBLICATION.** Reports of completed research or a major significant phase of research that present the results of NASA programs and include extensive data or theoretical analysis. Includes compilations of significant scientific and technical data and information deemed to be of continuing reference value. NASA's counterpart of peer-reviewed formal professional papers but has less stringent limitations on manuscript length and extent of graphic presentations.
- **TECHNICAL MEMORANDUM.** Scientific and technical findings that are preliminary or of specialized interest, e.g., quick release reports, working papers, and bibliographies that contain minimal annotation. Does not contain extensive analysis.
- **CONTRACTOR REPORT.** Scientific and technical findings by NASA-sponsored contractors and grantees.

- **CONFERENCE PUBLICATION.** Collected papers from scientific and technical conferences, symposia, seminars, or other meetings sponsored or cosponsored by NASA.
- **SPECIAL PUBLICATION.** Scientific, technical, or historical information from NASA programs, projects, and missions, often concerned with subjects having substantial public interest.
- **TECHNICAL TRANSLATION.** English-language translations of foreign scientific and technical material pertinent to NASA's mission.

Specialized services that complement the STI Program Office's diverse offerings include creating custom thesauri, building customized databases, organizing and publishing research results . . . even providing videos.

For more information about the NASA STI Program Office, see the following:

- Access the NASA STI Program Home Page at <http://www.sti.nasa.gov>
- E-mail your question via the Internet to help@sti.nasa.gov
- Fax your question to the NASA Access Help Desk at 301-621-0134
- Telephone the NASA Access Help Desk at 301-621-0390
- Write to:
NASA Access Help Desk
NASA Center for AeroSpace Information
7121 Standard Drive
Hanover, MD 21076



Benchmark Solutions for Computational Aeroacoustics (CAA) Code Validation

James R. Scott
Glenn Research Center, Cleveland, Ohio

Prepared for the
2004 International Mechanical Engineering Congress and RD&D Exposition
sponsored by the American Society of Mechanical Engineers
Anaheim, California, November 13–19, 2004

National Aeronautics and
Space Administration

Glenn Research Center

Acknowledgments

The author would like to thank Dr. Vladimir Golubev, Dr. Ray Hixon, Dr. David Kopriva, and Dr. Xiao-Yen Wang for their submissions to the CAA Workshops.

Available from

NASA Center for Aerospace Information
7121 Standard Drive
Hanover, MD 21076

National Technical Information Service
5285 Port Royal Road
Springfield, VA 22100

Available electronically at <http://gltrs.grc.nasa.gov>

Benchmark Solutions for Computational Aeroacoustics (CAA) Code Validation

James R. Scott

National Aeronautics and Space Administration
Glenn Research Center
Cleveland, Ohio 44135

Abstract

NASA has conducted a series of Computational Aeroacoustics (CAA) Workshops on Benchmark Problems to develop a set of realistic CAA problems that can be used for code validation. In the Third (1999) and Fourth (2003) Workshops, the single airfoil gust response problem, with real geometry effects, was included as one of the benchmark problems. Respondents were asked to calculate the airfoil RMS pressure and far-field acoustic intensity for different airfoil geometries and a wide range of gust frequencies. This paper presents the validated solutions that have been obtained to the benchmark problem, and in addition, compares them with classical flat plate results. It is seen that airfoil geometry has a strong effect on the airfoil unsteady pressure, and a significant effect on the far-field acoustic intensity. Those parts of the benchmark problem that have not yet been adequately solved are identified and presented as a challenge to the CAA research community.

Introduction

The validation of increasingly sophisticated CAA codes is one of the major challenges facing the CAA research community today. Recognizing this challenge, NASA has sponsored a series of Computational Aeroacoustics Workshops on Benchmark Problems [1-4], with the express purpose of developing a realistic set of validated CAA solutions that can be used for code validation.

A fundamental problem that has been included in all the Workshops to date is the gust response

problem. Initially, the focus was on flat plates, both for single airfoils and cascades. More recently, the focus has been on airfoils with real geometries. Included in this latter category is a problem that was submitted at the Third [3] and Fourth [4] Workshops, in which respondents were asked to calculate the aeroacoustic response of a 12% thick Joukowski airfoil to a periodic gust (for different airfoil geometries and gust frequencies).

The purpose of this paper is to present the validated solutions that have been obtained, and to identify those parts of the benchmark problem that have not yet been adequately solved. We also compare the validated results with those of classical thin airfoil theory, and show that airfoil geometry has a strong effect on the airfoil unsteady pressure, and a significant effect on the far-field acoustic intensity.

Benchmark Problem

Consider the airfoil configuration shown in Figure 1. The airfoil is two-dimensional with chord length c and angle of attack α . The upstream velocity is

$$\vec{U} = U_\infty \vec{i} + \vec{a} \cos[\vec{k} \cdot (\vec{x} - \vec{i} U_\infty t)] \quad (1)$$

where $\vec{x} = (x_1, x_2)$ denotes the spatial coordinates, $\vec{k} = (k_1, k_2)$ is the wave number vector, $\vec{a} = (a_1, a_2)$ is the gust amplitude vector with $a_1 = -\epsilon U_\infty k_2 / |\vec{k}|$, $a_2 = \epsilon U_\infty k_1 / |\vec{k}|$, and ϵ is a small parameter satisfying $\epsilon \ll 1$. Note that

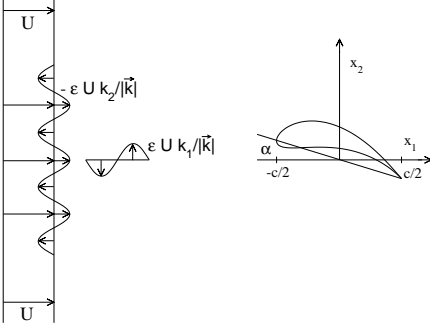


Figure 1 Airfoil in a two-dimensional gust.

\vec{a} and \vec{k} satisfy $\vec{a} \cdot \vec{k} = 0$, and that \vec{k} specifies the direction of gust propagation.

The governing equations are the 2-D Euler equations

$$\frac{\partial \rho}{\partial t} + \frac{\partial}{\partial x}(\rho u) + \frac{\partial}{\partial y}(\rho v) = 0 \quad (2)$$

$$\frac{\partial}{\partial t}(\rho u) + \frac{\partial}{\partial x}(\rho u^2 + p) + \frac{\partial}{\partial y}(\rho u v) = 0 \quad (3)$$

$$\frac{\partial}{\partial t}(\rho v) + \frac{\partial}{\partial x}(\rho u v) + \frac{\partial}{\partial y}(\rho v^2 + p) = 0 \quad (4)$$

$$\frac{\partial E_t}{\partial t} + \frac{\partial}{\partial x}[(E_t + p)u] + \frac{\partial}{\partial y}[(E_t + p)v] = 0 \quad (5)$$

where ρ , u , v , p and E_t denote the fluid density, x and y velocity, pressure, and total internal energy per unit volume. The system is closed using the perfect gas equation of state. Flow variables are nondimensionalized as follows:

x_1, x_2	by	$\frac{c}{2}$
$\vec{U} = (u, v)$	by	U_∞
c_0 (sound speed)	by	U_∞
ρ	by	ρ_∞
p	by	$\rho_\infty U_\infty^2$
T (temperature)	by	T_∞
t (time)	by	$\frac{c}{2U_\infty}$
$\omega = k_1 U_\infty$ (gust angular frequency)	by	$\frac{2}{c}$
k_1, k_2	by	$\frac{2}{c}$

The nondimensional parameter $\frac{\omega c}{2U_\infty} = k_1$ is called the reduced frequency.

For the following two cases, respondents are asked to solve the gust response problem for a Joukowski airfoil in a two-dimensional gust with $k_2 = k_1$, for reduced frequencies $k_1 = 0.1$, 1.0 , 2.0 , and 3.0 . The nondimensional upstream velocity is $\vec{U} = \vec{i} + \epsilon \vec{a} \cos(\vec{k} \cdot \vec{x} - k_1 t)$, where $\vec{a} = (a_1, a_2) = (-\frac{\sqrt{2}}{2}, \frac{\sqrt{2}}{2})$. Take $\epsilon = 0.02$.

For Case 1, the airfoil has a 12% thickness ratio, free stream Mach number $M_\infty = 0.5$, angle of attack $\alpha = 0^\circ$, and a camber ratio of zero.

For Case 2, change α to 2° and the camber ratio to 0.02.

The airfoil geometries can be generated as follows. Set

$$\zeta_1 = r_0 e^{i\theta} + \zeta_0 \quad (6)$$

where

$$\zeta_0' = -\epsilon_1 + i\epsilon_2 \quad (7)$$

is a complex constant. Letting $z = x + iy$ denote the airfoil coordinates in the complex z plane, the transformation

$$z = \left(\zeta_1 + \frac{d^2}{\zeta_1} \right) e^{-i\alpha} \quad (8)$$

transforms the ζ_1 circle defined by equation (6) into the desired airfoil shape.

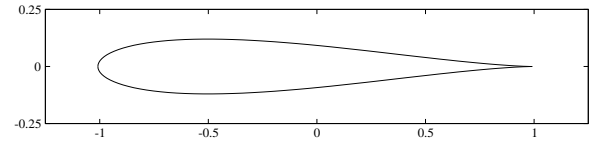


Figure 2.a Symmetric Joukowski airfoil with 12% thickness ratio and zero degree angle of attack. (Case 1)

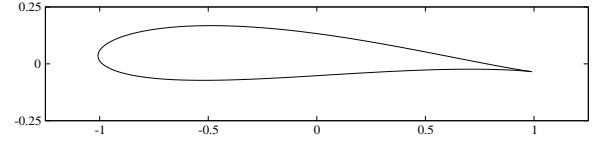


Figure 2.b Joukowski airfoil with 12% thickness ratio, 2% camber, and 2 degree angle of attack. (Case 2)

For Case 1, use $r_0 = 0.54632753$, $\epsilon_1 = 0.05062004$, $\epsilon_2 = 0$, $d^2 = 0.24572591$, $\alpha = 0$. All parameters are specified to eight decimals to ensure that the airfoil geometry is precisely defined. Discretize the ζ_1 circle in θ , starting from 0 and going to 2π , and then apply equation (8) to get the airfoil coordinates. The values $\theta = 0$ and $\theta = 2\pi$ map into the trailing edge point.

For Case 2, use $r_0 = 0.54676443$, $\epsilon_1 = 0.05062004$, $\epsilon_2 = 0.02185310$, $d^2 = 0.24572591$, $\alpha = 0.034906585$. Discretize the ζ_1 circle in θ , starting from $\theta = -\beta$ and going to $\theta = 2\pi - \beta$, where $\beta = 0.039978687$, and then apply equation (8) to

get the airfoil coordinates. The values $\theta = -\beta$ and $\theta = 2\pi - \beta$, map into the trailing edge point.

The above procedure will generate a Joukowski airfoil of chord length 2, situated very nearly between $x = -1$ and $x = 1$. The airfoil geometries are shown in Figure 2.

For both Case 1 and Case 2, respondents are asked to march the discrete equations in time until the solution becomes periodic. On the airfoil surface, calculate the RMS pressure $\sqrt{\langle p' \rangle^2}$. In the far field, calculate the intensity $\langle p' \rangle^2$ on a circle centered about the airfoil center for the following three circle radii: (i) $R = 2$ (one chord length); (ii) $R = 4$ (two chord lengths); (iii) $R = 8$ (four chord lengths).

Linearized Benchmark Solution

Since the gust amplitude is small, the solution can be obtained from the linearized Euler equations. Let the flow field be decomposed according to

$$\vec{U}(\vec{x}, t) = \vec{U}_0(\vec{x}) + \vec{u}(\vec{x}, t) \quad (9)$$

$$p(\vec{x}, t) = p_0(\vec{x}) + p'(\vec{x}, t) \quad (10)$$

$$\rho(\vec{x}, t) = \rho_0(\vec{x}) + \rho'(\vec{x}, t) \quad (11)$$

$$s(\vec{x}, t) = s_0 + s'(\vec{x}, t) \quad (12)$$

where the entropy s_0 is constant, and \vec{u} , p' , ρ' , and s' are the unsteady perturbation velocity, pressure, density and entropy, respectively. Mean flow quantities are denoted by zero subscripts and are assumed to be known.

Substituting (9) – (12) into the nonlinear Euler equations and neglecting products of small quantities, one obtains the linearized equations

$$\frac{D_0 \rho'}{Dt} + \rho' \vec{\nabla} \cdot \vec{U}_0 + \vec{\nabla} \cdot (\rho_0 \vec{u}) = 0 \quad (13)$$

$$\rho_0 \left(\frac{D_0 \vec{u}}{Dt} + \vec{u} \cdot \vec{\nabla} \vec{U}_0 \right) + \rho' \vec{U}_0 \cdot \vec{\nabla} \vec{U}_0 = -\vec{\nabla} p' \quad (14)$$

$$\frac{D_0 s'}{Dt} = 0, \quad (15)$$

where $\frac{D_0}{Dt} = \frac{\partial}{\partial t} + \vec{U}_0 \cdot \vec{\nabla}$ is the convective derivative associated with the mean flow.

In the present problem, the mean velocity \vec{U}_0 can be expressed as the gradient of a potential Φ_0 . Therefore, equations (13) - (15) can be reduced to the single convective wave equation [5,6]

$$\frac{D_0}{Dt} \left(\frac{1}{c_0^2} \frac{D_0 \phi}{Dt} \right) - \frac{1}{\rho_0} \vec{\nabla} \cdot (\rho_0 \vec{\nabla} \phi) = \frac{1}{\rho_0} \vec{\nabla} \cdot (\rho_0 \vec{u}^{(R)}), \quad (16)$$

where the unsteady velocity is decomposed into a known vortical component $\vec{u}^{(R)}$ and an unknown potential component $\vec{\nabla} \phi$,

$$\vec{u}(\vec{x}, t) = \vec{u}^{(R)} + \vec{\nabla} \phi. \quad (17)$$

The unsteady pressure is given by

$$p' = -\rho_0(\vec{x}) \frac{D_0 \phi}{Dt}. \quad (18)$$

An unsteady aerodynamic code, called GUST3D [7], has been developed to solve equation (16) for flows with periodic vortical disturbances. The code uses a frequency domain approach with second-order central differences and a pressure radiation condition in the far field [8]. GUST3D requires as input certain mean flow quantities which are calculated separately by a potential flow solver. This solver calculates the mean flow for interior mesh points using a Gothert's Rule approximation [7]. On the airfoil surface, where the Gothert's Rule approximation is no longer valid, GUST3D uses the potential flow solution calculated by FLO36 [9].

Recently, GUST3D was upgraded to include a domain decomposition approach [10]. This has led to significant improvements in accuracy. Both versions of the code were used to obtain the benchmark solutions presented at the Fourth Workshop and in this paper.

Finally, we employ a Kirchoff method [11] to obtain the intensity results on the circle of radius four chord lengths. The Kirchoff surface is the circle of radius two chord lengths. This approach has proven to increase accuracy in far-field pressure calculations.

Benchmark Results

In Figs. 3 - 19 we present the benchmark results. Figures 3 - 9 present the RMS airfoil pressure, and Figs. 10 - 19 present the acoustic intensity on circles of radius one and four chord lengths. For brevity, we omit the intensity results for the circle of radius two chord lengths. These results essentially paralleled the other intensity results. The flat plate RMS results shown in Figs. 3.b - 9.b were obtained from a Possio solver [12,13], and the flat plate intensity results shown in Figs. 10.b - 19.b were obtained by the method of Atassi et al [13]. In each figure, the flat plate solution is shown versus a representative benchmark solution. Only one benchmark solution is shown for clarity.

The benchmark results selected for each figure represent the best solutions available from the Third

and Fourth Workshops. Along with the GUST3D code, the results are from the PFC6 code of Hixon et al [14-16], the CE/SE code of Wang et al [17,18,4], the DSEM code of Rasetarinera et al [19,20], the BASS code [21-23,4], and the STMA code [24,4]. It is worth noting that the above codes are all based on fundamentally different algorithms, except for BASS, which is an upgraded version of PFC6. All the codes, except GUST3D, are nonlinear Euler solvers. The agreement between the codes ranges from good to excellent for most of the figures. It should be noted that when results from a particular code are not shown, it means either no solution was available or that the solution did not agree well with the other codes.

From Figs. 3.b - 9.b, it is clear that airfoil geometry has a very strong effect on the unsteady pressure. The flat plate solutions differ markedly from the Joukowski airfoil solutions in every case. For the flat plate, the strong leading edge singularity is clearly visible, whereas for the thick airfoil, there is only a pressure spike due to the rounded leading edge. Note that the flat plate RMS pressure is identical on both sides of the airfoil, whereas the RMS pressure for the Joukowski airfoil differs from one side to the other. This is due to the airfoil thickness and the fact that the gust propagates at a 45° angle i.e., $k_2 = k_1$.

From Figs. 10.b - 19.b, one observes substantial differences between the intensity profiles for the Joukowski airfoils versus the flat plate. As expected, the differences tend to diminish somewhat on the four-chord-length circle, where the mean flow is nearly uniform. However, even at this distance, there are still substantial differences for some cases.

The tables below summarize the benchmark problem and the validated solutions that have been

obtained. In spite of the rather large number of validated solutions, it is clear from Tables I and II that more work remains to be done. The high frequency cases $k_1 = 2.0$ and 3.0 indeed pose a significant challenge, for a number of reasons. First, the incoming gust must be propagated accurately all the way from the upstream boundary to the airfoil. For the high frequency/short wavelength cases, this requires a fine mesh in the far field, leading to many more mesh points and much longer solution times. Second, radiation boundary conditions typically lose accuracy at the higher reduced frequencies, making it more difficult to obtain an accurate solution. Finally, for high reduced frequency cases, there is a stronger interaction between the mean flow and the convected gust, leading to a more challenging physical problem.

Conclusion

This paper presents a new set of validated CAA solutions to the single airfoil gust response problem. The results were obtained from NASA's Third and Fourth Computational Aeroacoustics Workshops on Benchmark Problems held in 1999 and 2003. All together, the solutions come from six different CAA codes, five of which are full Euler solvers. Good to excellent agreement is demonstrated in the airfoil RMS pressures and far-field acoustic intensities for different reduced frequencies and airfoil geometries. Comparison with classical flat plate solutions shows that airfoil geometry has a strong effect on the RMS airfoil pressure, and a significant effect on the far-field acoustic intensity. Further work is needed to obtain accurate results for the high reduced frequency cases $k_1 = 2.0$ and 3.0 . These cases are presented to the CAA research community as a challenge yet to be completed.

	AF Pressure	Intensity, $R=1c$	Intensity, $R=4c$
k_1			
0.1	GUST3D,PFC6, CE/SE,STMA	GUST3D,BASS, CE/SE,STMA	GUST3D,BASS, CE/SE,STMA
1.0	GUST3D,DSEM, CE/SE	GUST3D,BASS, CE/SE,STMA	GUST3D,STMA, CE/SE,DSEM
2.0	GUST3D,BASS	XXXXXXXXXX	XXXXXXXXXX
3.0	GUST3D,DSEM CE/SE	CE/SE	DSEM,CE/SE

Table I Solution matrix for Case 1.

	AF Pressure	Intensity, $R=1c$	Intensity, $R=4c$
k_1			
0.1	GUST3D,PFC6, CE/SE,STMA	GUST3D,BASS, CE/SE,STMA	GUST3D,BASS, CE/SE,STMA
1.0	DSEM,CE/SE	BASS,CE/SE, STMA	BASS,CE/SE, STMA,DSEM
2.0	GUST3D,BASS	XXXXXXXXXX	XXXXXXXXXX
3.0	XXXXXXXXXX	XXXXXXXXXX	XXXXXXXXXX

Table II Solution matrix for Case 2.

REFERENCES

1. Hardin, J.C., Ristorcelli, J.R., and Tam, C.K.W. eds., 1995, ICASE/LaRC Workshop on Benchmark Problems in Computational Aeroacoustics (CAA), Proceedings of a workshop sponsored by NASA and the Institute for Computer Applications in Science and Engineering (ICASE), Hampton, Virginia, and held in Hampton, Virginia, Oct. 24-26, 1994, NASA/CP-3300.
2. Tam, C.K.W. and Hardin, J.C. eds., 1997, Second Computational Aeroacoustics (CAA) Workshop on Benchmark Problems, Proceedings of a workshop sponsored by NASA and the Florida State University, Tallahassee, Florida, and held in Tallahassee, Florida, Nov. 4-5, 1996, NASA/CP-3352.
3. Dahl, M.D., ed., 2000, Third Computational Aeroacoustics (CAA) Workshop on Benchmark Problems, Proceedings of a conference held at and sponsored by NASA and the Ohio Aerospace Institute, Cleveland, Ohio, Nov. 8-10, 1999, NASA/CP-2000-209790.
4. Dahl, M.D., ed., (to appear 2004), Fourth Computational Aeroacoustics (CAA) Workshop on Benchmark Problems, Proceedings of a conference held at and sponsored by NASA and the Ohio Aerospace Institute, Cleveland, Ohio, Oct. 20-22, 2003.
5. M.E. Goldstein, 1978, "Unsteady vortical and entropic distortions of potential flows round arbitrary obstacles," *J. Fluid Mech.*, **89**, pp. 433-468.
6. H.M. Atassi and J. Grzedzinski, 1989, "Unsteady disturbances of streaming motions around bodies," *J. Fluid Mech.*, **209**, pp. 385-403.
7. J.R. Scott and H.M. Atassi, 1995, "A Finite-Difference, Frequency-Domain Numerical Scheme for the Solution of the Gust Response Problem," *J. Comp. Phys.*, **119**, pp. 75-93.
8. J.R. Scott, K.L. Kreider and J.A. Heminger, 2004, "Evaluation of Radiation Boundary Conditions for the Gust Response Problem," *AIAA Journal*, **42**, No. 2, pp. 249-254.
9. A. Jameson and D.A. Caughey, 1979, "A Finite Volume Method for Transonic Potential Flow Calculations," Proceedings of the AIAA 3rd Computational Fluid Dynamics Conference, Williamsburg, Virginia, p. 122.
10. J.R. Scott, H.M. Atassi, and R.F. Susan-Resiga, 2003, "A New Domain Decomposition Approach for the Gust Response Problem," *AIAA Paper 2003-0883*.
11. S.I. Hariharan, J.R. Scott and K.L. Kreider, 2000, "A Potential-Theoretic Method for Far-Field Sound Radiation Calculations," *J. Comp. Phys.*, **164**, pp. 143-164.
12. Possio, C., 1938, "L'Azione Aerodinamica sul Profilo Oscillante in un Fluido Compressibile a Velocita Isonora, L'Aerotecnica, **XVIII**, fasc. 4.
13. Atassi, H.M., Dusey, M., and Davis, C.M., 1993, "Acoustic Radiation from a Thin Airfoil in Nonuniform Subsonic Flows," *AIAA Journal*, **31**, No. 1, pp. 12-19.
14. Hixon, R., Shih, S.-H., Mankbadi R.R., and Scott, J.R., 1998, "Time Domain Solution of the Airfoil Gust Problem Using a High-Order Compact Scheme," *AIAA Paper 98-3241*.
15. Hixon, R. and Mankbadi, R.R., 2000, "Validation of a High-Order Prefactored Compact Scheme on Nonlinear Flows With Complex Geometries", Third Computational Aeroacoustics (CAA) Workshop on Benchmark Problems, Proceedings of a conference held at and sponsored by NASA and the Ohio Aerospace Institute, Cleveland, Ohio, M.D. Dahl, ed., Nov. 8-10, 1999, NASA/CP-2000-209790, pp. 117-132.
16. Hixon, R., Mankbadi R.R., and Scott, J.R., 2001, "Validation of a High-Order Prefactored Compact Code on Nonlinear Flows with Complex Geometries," *AIAA Paper 2001-1103*.
17. Wang, X.-Y., Himansu, A., Chang, S.-C., and Jorgenson, P.C.E., 2000, "Applications of the Space-Time Conservation Element and Solution Element (CE/SE) Method to Computational Aeroacoustic Benchmark Problems," Third Computational Aeroacoustics (CAA) Workshop on Benchmark Problems, Proceedings of a conference held at and sponsored by NASA and the Ohio Aerospace Institute, Cleveland, Ohio, M.D. Dahl, ed., Nov. 8-10, 1999, NASA/CP-2000-209790, pp. 133-159.
18. Wang, X.Y., Chang, S.C., Himansu, A., and Jorgenson, P., 2002, "Gust Acoustic Response of a Single Airfoil Using the Space-Time CE/SE Method," *AIAA Paper 2002-0801*.

19. Rasetarinera, P., Kopriva, D.A., and Hussaini, M.Y., 2000, "Discontinuous Spectral Element Solution of Aeroacoustic Problems," Third Computational Aeroacoustics (CAA) Workshop on Benchmark Problems, Proceedings of a conference held at and sponsored by NASA and the Ohio Aerospace Institute, Cleveland, Ohio, M.D. Dahl, ed., Nov. 8-10, 1999, NASA/CP-2000-209790, pp. 103-115.
20. Rasetarinera, P., Kopriva, D.A., and Hussaini, M.Y., 2001, "Discontinuous Spectral Element Solution of Acoustic Radiation from Thin Airfoils," AIAA Journal, **39**, No. 11, pp. 2070-2075.
21. Hixon, R., Nallasamy, M., and Sawyer, S.S., 2002, "Parallelization Strategy for an Explicit Computational Aeroacoustic Code," AIAA Paper 2002-2583.
22. Crivellini, A., Golubev, V., Mankbadi R.R., Scott, J.R., Hixon, R., and Povinelli, L.A., 2002, "Nonlinear Analysis of Airfoil High-Intensity Gust Response Using a High-Order Prefactored Compact Code," AIAA Paper 2002-2535.
23. Golubev, V.V., Mankbadi R.R., and Scott, J.R., 2004, "Numerical Inviscid Analysis of Nonlinear Airfoil Response to Impinging High-Intensity High-Frequency Gust," AIAA Paper 2004-3002.
24. Hixon, R., "Space-Time Mapping Analysis for the Accurate Calculation of Complex Unsteady Flows," AIAA Paper 2003-3205, May, 2003.

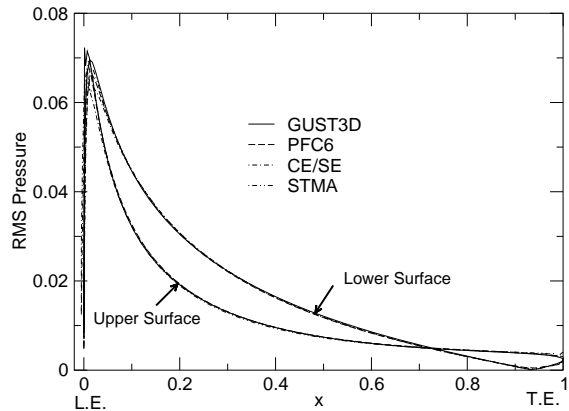


Figure 3.a RMS pressure on airfoil surface,
symmetric airfoil, $k_1=k_2=0.1$

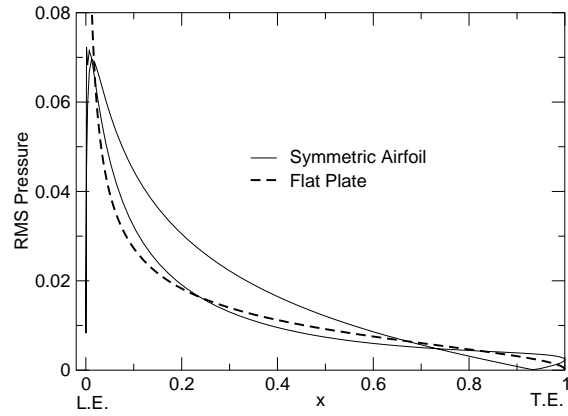


Figure 3.b Symmetric airfoil solution (GUST3D)
versus flat plate solution, $k_1=k_2=0.1$

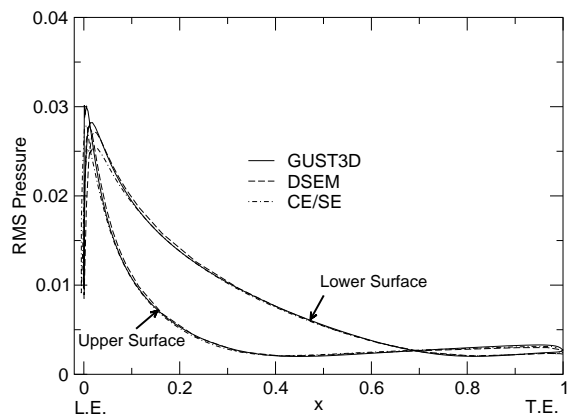


Figure 4.a RMS pressure on airfoil surface,
symmetric airfoil, $k_1=k_2=1.0$

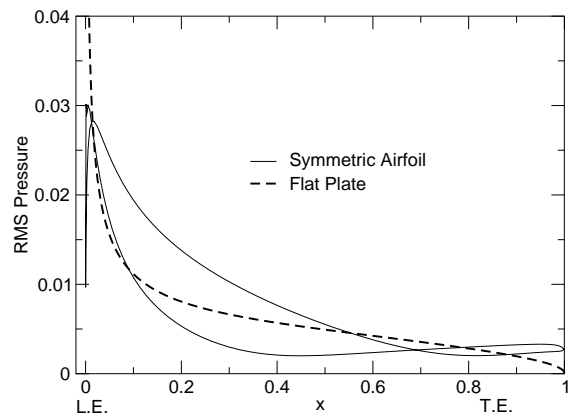


Figure 4.b Symmetric airfoil solution (GUST3D)
versus flat plate solution, $k_1=k_2=1.0$

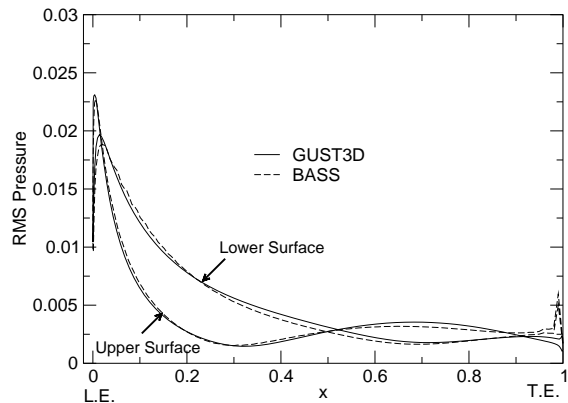


Figure 5.a RMS pressure on airfoil surface,
symmetric airfoil, $k_1=k_2=2.0$

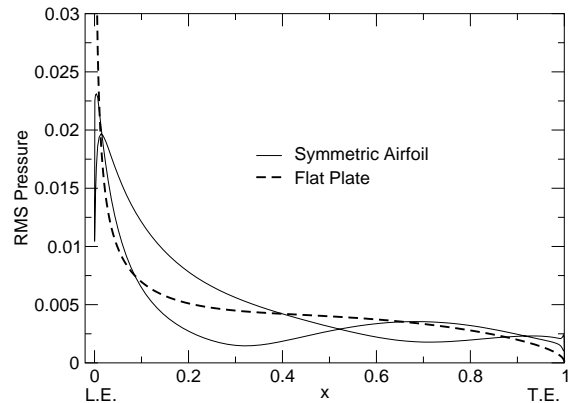


Figure 5.b Symmetric airfoil solution (GUST3D)
versus flat plate solution, $k_1=k_2=2.0$

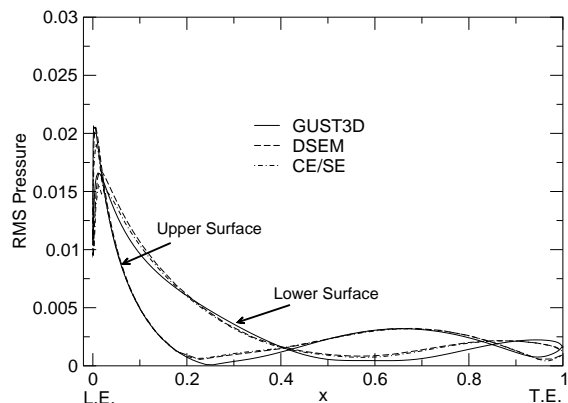


Figure 6.a RMS pressure on airfoil surface,
symmetric airfoil, $k_1=k_2=3.0$

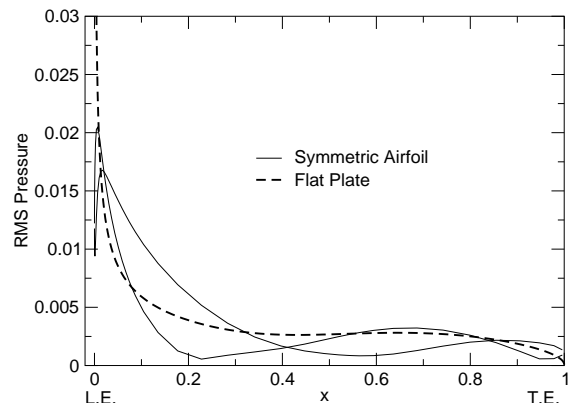


Figure 6.b Symmetric airfoil solution (DSEM)
versus flat plate solution, $k_1=k_2=3.0$

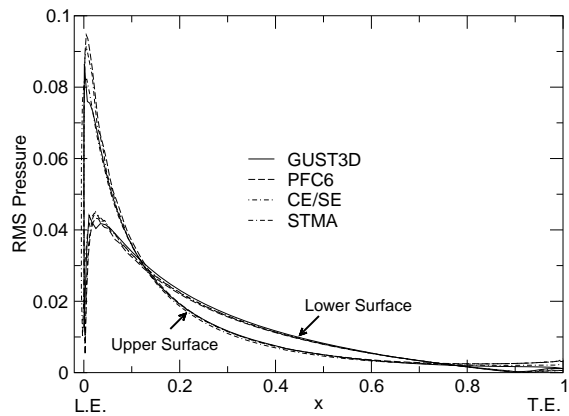


Figure 7.a RMS pressure on airfoil surface, cambered airfoil, $k_1=k_2=0.1$

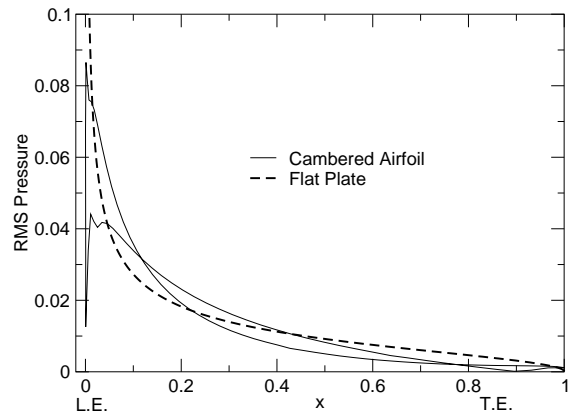


Figure 7.b Cambered airfoil solution (GUST3D) versus flat plate solution, $k_1=k_2=0.1$

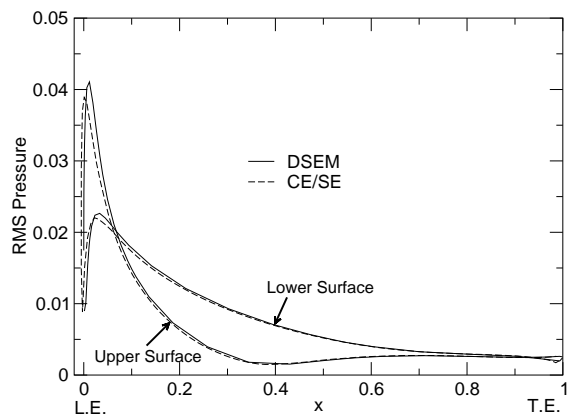


Figure 8.a RMS pressure on airfoil surface, cambered airfoil, $k_1=k_2=1.0$

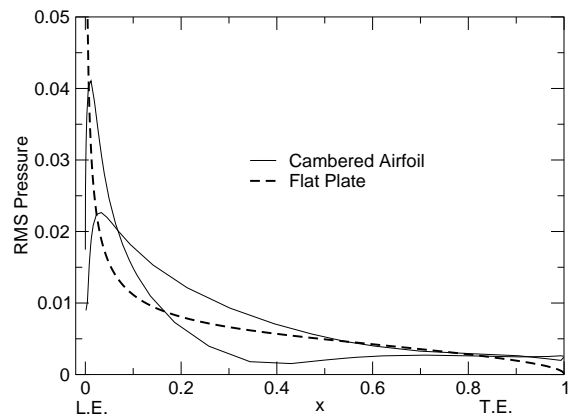


Figure 8.b Cambered airfoil solution (DSEM) versus flat plate solution, $k_1=k_2=1.0$

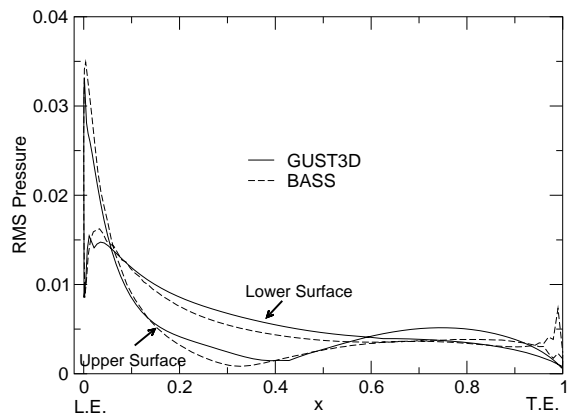


Figure 9.a RMS pressure on airfoil surface, cambered airfoil, $k_1=k_2=2.0$

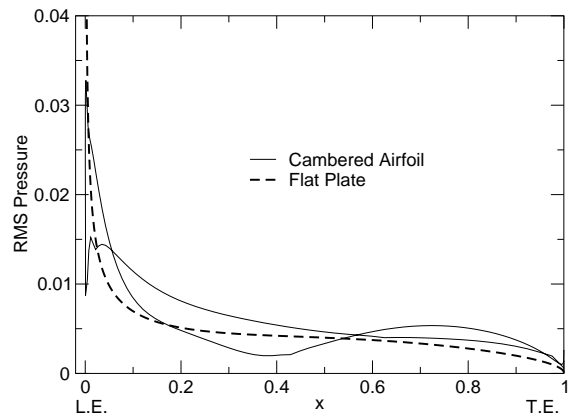


Figure 9.b Cambered airfoil solution (GUST3D) versus flat plate solution, $k_1=k_2=2.0$

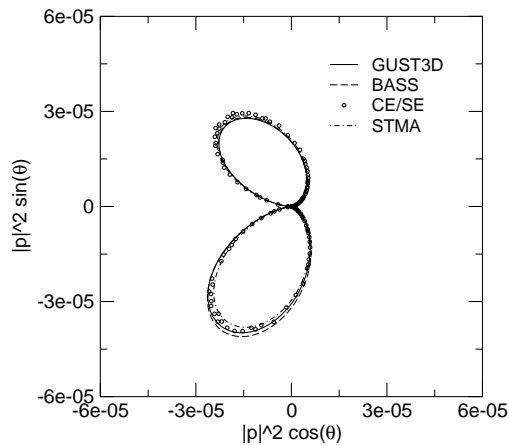


Figure 10.a Acoustic intensity on circle $R = 1c$,
symmetric airfoil, $k_1 = k_2 = 0.1$

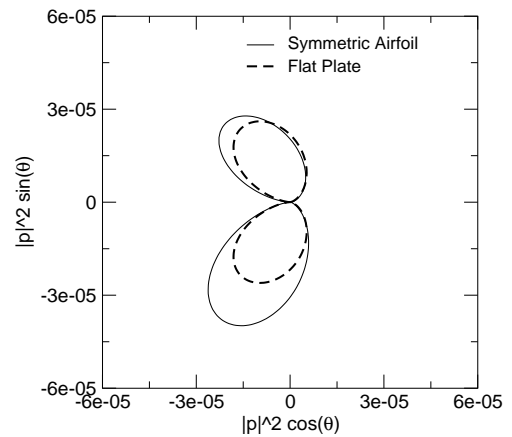


Figure 10.b Symmetric airfoil solution (GUST3D)
versus flat plate solution on circle $R = 1c$, $k_1 = k_2 = 0.1$

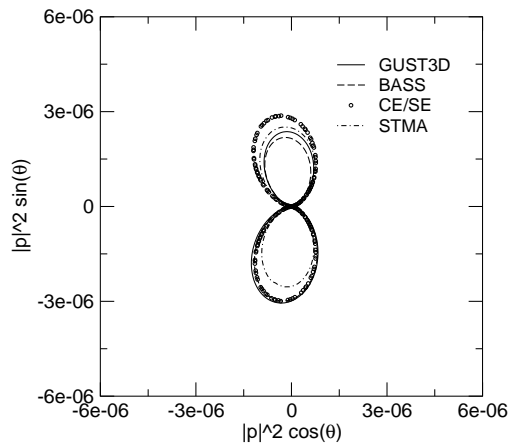


Figure 11.a Acoustic intensity on circle $R = 4c$,
symmetric airfoil, $k_1 = k_2 = 0.1$

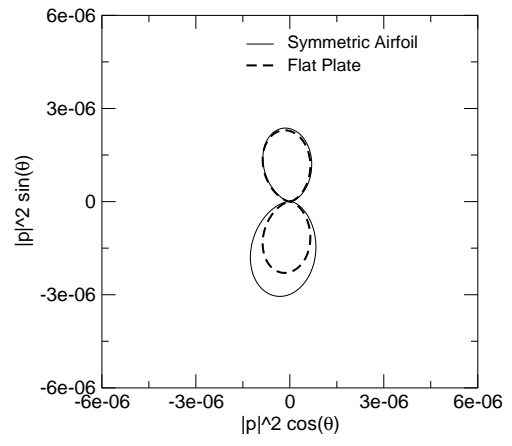


Figure 11.b Symmetric airfoil solution (GUST3D)
versus flat plate solution on circle $R = 4c$, $k_1 = k_2 = 0.1$

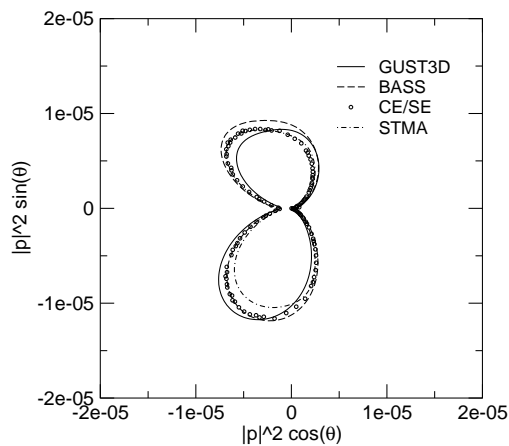


Figure 12.a Acoustic intensity on circle $R = 1c$,
symmetric airfoil, $k_1 = k_2 = 1.0$

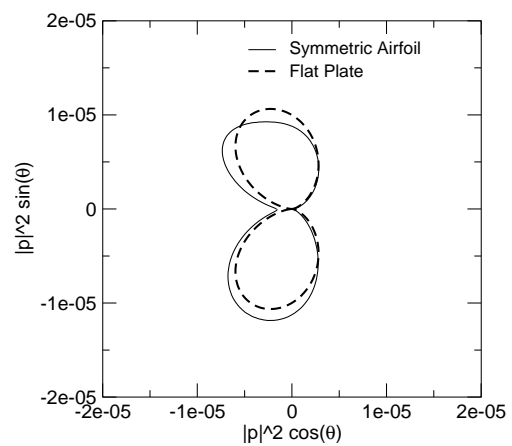


Figure 12.b Symmetric airfoil solution (BASS)
versus flat plate solution on circle $R = 1c$, $k_1 = k_2 = 1.0$

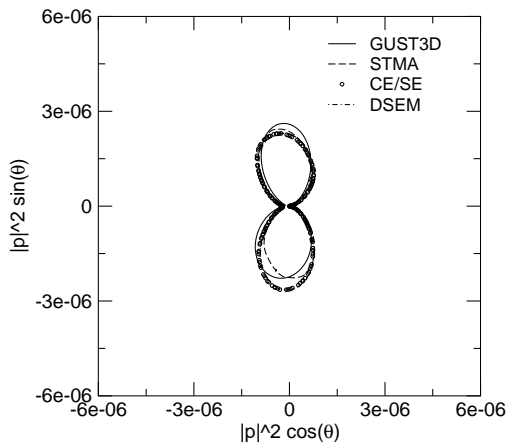


Figure 13.a Acoustic intensity on circle $R=4c$,
symmetric airfoil, $k_1=k_2=1.0$

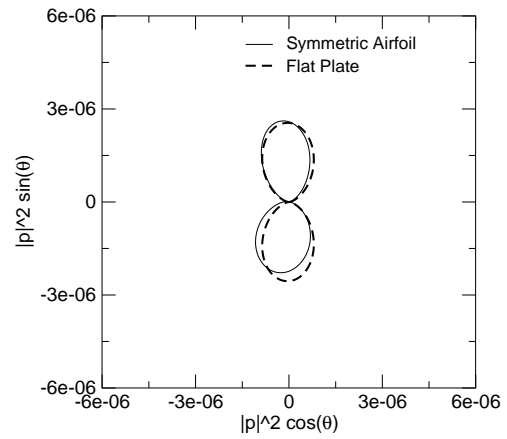


Figure 13.b Symmetric airfoil solution (GUST3D)
versus flat plate solution on circle $R=4C$, $k_1=k_2=1.0$

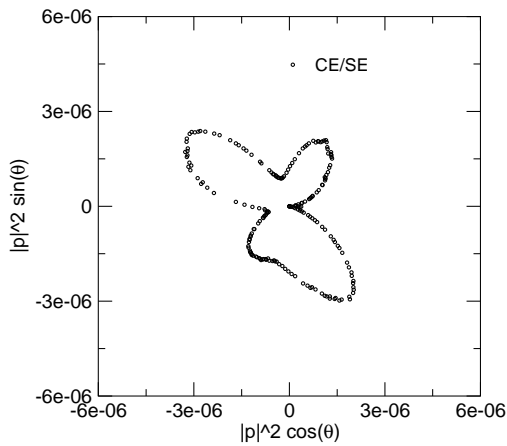


Figure 14.a Acoustic intensity on circle
 $R=1c$, symmetric airfoil, $k_1=k_2=3.0$

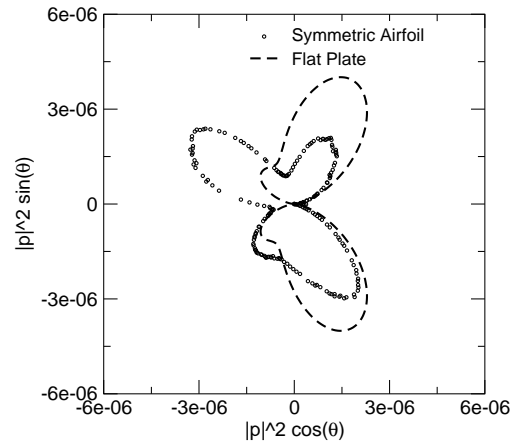


Figure 14.b Symmetric airfoil solution (CE/SE)
versus flat plate solution on circle $R=1c$, $k_1=k_2=3.0$

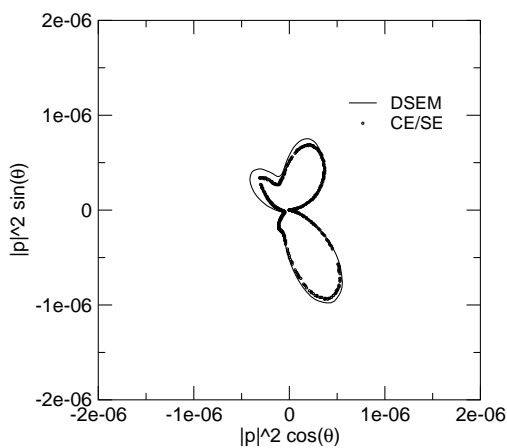


Figure 15.a Acoustic intensity on circle $R=4c$,
symmetric airfoil, $k_1=k_2=3.0$

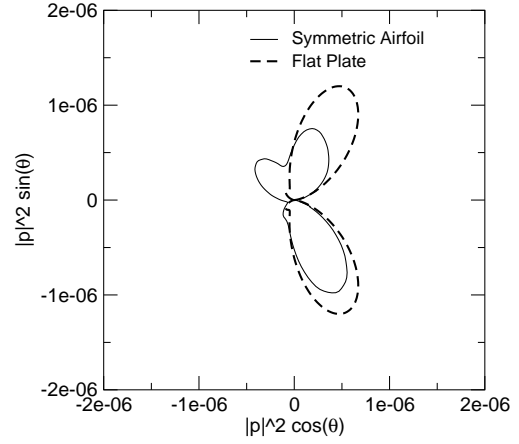


Figure 15.b Symmetric airfoil solution (DSEM)
versus flat plate solution on circle $R=4c$, $k_1=k_2=3.0$

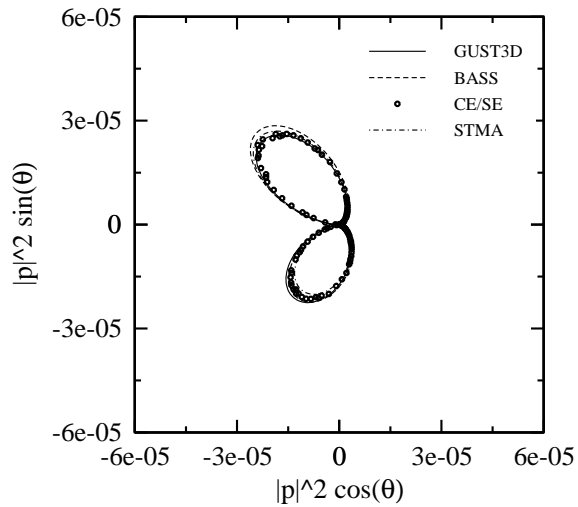


Figure 16.a Acoustic intensity on circle
 $R=1c$, cambered airfoil, $k_1=k_2=0.1$

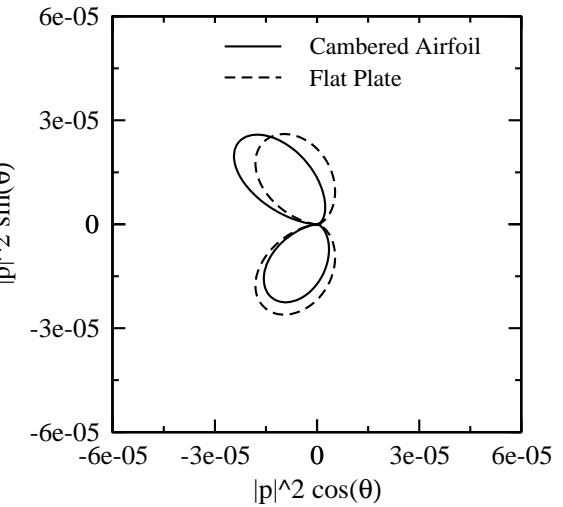


Figure 16.b Cambered airfoil solution (GUST3D)
versus flat plate solution on circle $R=1c$, $k_1=k_2=0.1$

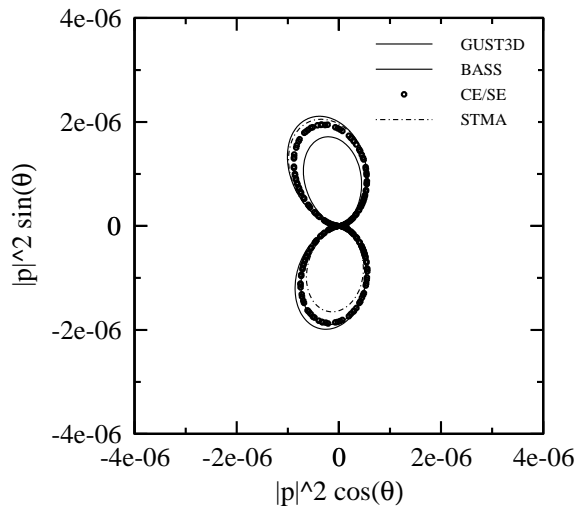


Figure 17.a Acoustic intensity on circle
 $R=4c$, cambered airfoil, $k_1=k_2=0.1$

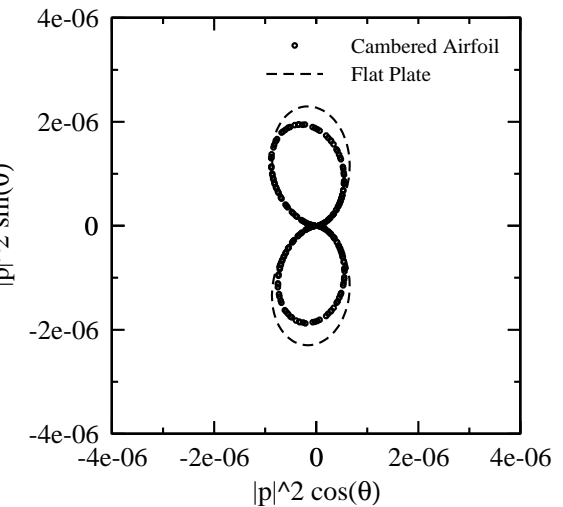


Figure 17.b Cambered airfoil solution (CE/SE)
versus flat plate solution on circle $R=4c$, $k_1=k_2=0.1$

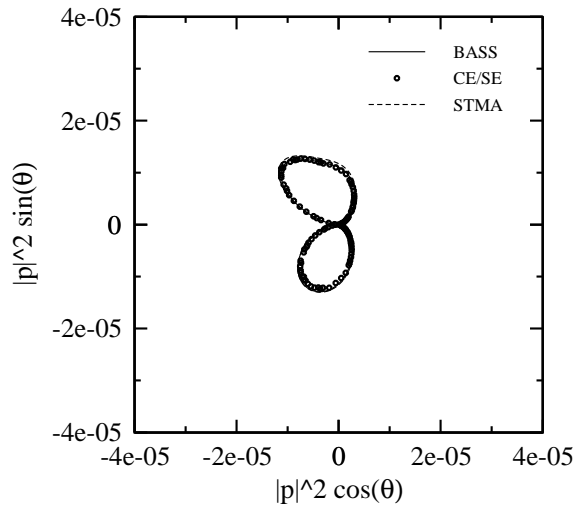


Figure 18.a Acoustic intensity on circle
 $R=1c$, cambered airfoil, $k_1=k_2=1.0$

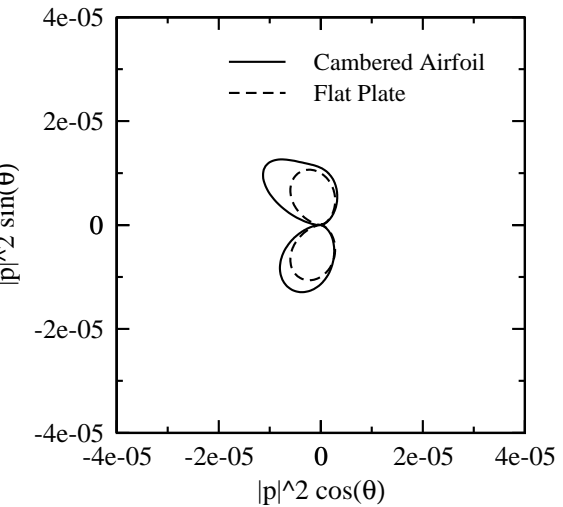


Figure 18.b Cambered airfoil solution (BASS)
versus flat plate solution on circle $R=1c$, $k_1=k_2=1.0$

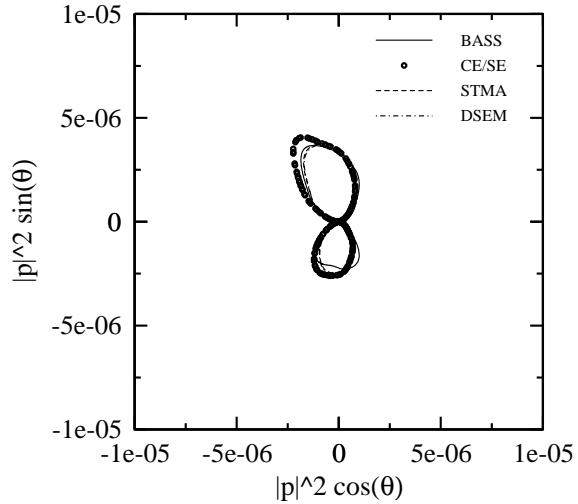


Figure 19.a Acoustic intensity on circle
 $R=4c$, cambered airfoil, $k_1=k_2=1.0$

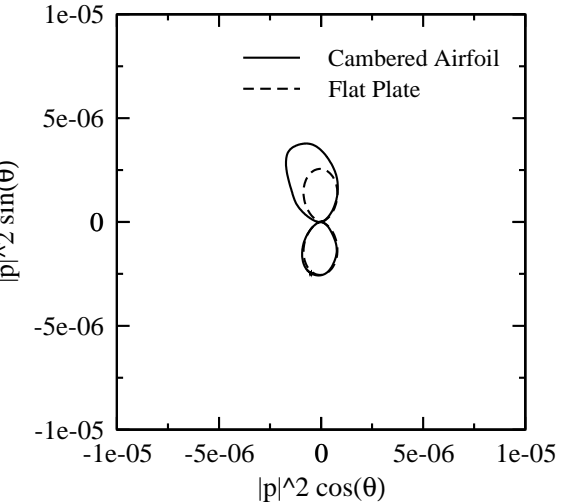


Figure 19.b Cambered airfoil solution (STMA)
versus flat plate solution on circle $R=4c$, $k_1=k_2=1.0$

REPORT DOCUMENTATION PAGE			<i>Form Approved OMB No. 0704-0188</i>
Public reporting burden for this collection of information is estimated to average 1 hour per response, including the time for reviewing instructions, searching existing data sources, gathering and maintaining the data needed, and completing and reviewing the collection of information. Send comments regarding this burden estimate or any other aspect of this collection of information, including suggestions for reducing this burden, to Washington Headquarters Services, Directorate for Information Operations and Reports, 1215 Jefferson Davis Highway, Suite 1204, Arlington, VA 22202-4302, and to the Office of Management and Budget, Paperwork Reduction Project (0704-0188), Washington, DC 20503.			
1. AGENCY USE ONLY (Leave blank)	2. REPORT DATE	3. REPORT TYPE AND DATES COVERED	
	December 2004	Technical Memorandum	
4. TITLE AND SUBTITLE		5. FUNDING NUMBERS	
Benchmark Solutions for Computational Aeroacoustics (CAA) Code Validation		WBS-22-781-30-09	
6. AUTHOR(S)		7. PERFORMING ORGANIZATION NAME(S) AND ADDRESS(ES)	
James R. Scott		National Aeronautics and Space Administration John H. Glenn Research Center at Lewis Field Cleveland, Ohio 44135-3191	
8. PERFORMING ORGANIZATION REPORT NUMBER		9. SPONSORING/MONITORING AGENCY NAME(S) AND ADDRESS(ES)	
E-14894		National Aeronautics and Space Administration Washington, DC 20546-0001	
10. SPONSORING/MONITORING AGENCY REPORT NUMBER		11. SUPPLEMENTARY NOTES	
NASA TM-2004-213386 IMECE2004-59865		Prepared for the 2004 International Mechanical Engineering Congress and RD&D Exposition sponsored by the American Society of Mechanical Engineers, Anaheim, California, November 13-19, 2004. Responsible person, James R. Scott, organization code, 5940, 216-433-5863.	
12a. DISTRIBUTION/AVAILABILITY STATEMENT		12b. DISTRIBUTION CODE	
Unclassified - Unlimited Subject Categories: 02 and 71 Available electronically at http://gltrs.grc.nasa.gov This publication is available from the NASA Center for AeroSpace Information, 301-621-0390.		Distribution: Nonstandard	
13. ABSTRACT (Maximum 200 words)			
NASA has conducted a series of Computational Aeroacoustics (CAA) Workshops on Benchmark Problems to develop a set of realistic CAA problems that can be used for code validation. In the Third (1999) and Fourth (2003) Workshops, the single airfoil gust response problem, with real geometry effects, was included as one of the benchmark problems. Respondents were asked to calculate the airfoil RMS pressure and far-field acoustic intensity for different airfoil geometries and a wide range of gust frequencies. This paper presents the validated that have been obtained to the benchmark problem, and in addition, compares them with classical flat plate results. It is seen that airfoil geometry has a strong effect on the airfoil unsteady pressure, and a significant effect on the far-field acoustic intensity. Those parts of the benchmark problem that have not yet been adequately solved are identified and presented as a challenge to the CAA research community.			
14. SUBJECT TERMS		15. NUMBER OF PAGES	
Unsteady aerodynamics; Euler equations of motion; Gusts; Noise prediction (aircraft); Aircraft noise; Aeroacoustics; Computational fluid dynamics		19	
		16. PRICE CODE	
17. SECURITY CLASSIFICATION OF REPORT	18. SECURITY CLASSIFICATION OF THIS PAGE	19. SECURITY CLASSIFICATION OF ABSTRACT	20. LIMITATION OF ABSTRACT
Unclassified	Unclassified	Unclassified	

